J|A|C|S COMMUNICATIONS

Published on Web 07/22/2010

Photoswitchable Catalysis Mediated by Dynamic Aggregation of Nanoparticles

Yanhu Wei, Shuangbing Han, Jiwon Kim, Siowling Soh, and Bartosz A. Grzybowski*

Department of Chemistry and Department of Chemical and Biological Engineering, Northwestern University, 2145 Sheridan Road, Evanston, Illinois 60208-3113

Received May 26, 2010; E-mail: grzybor@northwestern.edu

Abstract: Catalytic activity of gold nanoparticles in a hydrosilylation reaction is controlled by irradiation with UV or visible light. When exposed to UV, the particles aggregate and the catalysis is effectively switched "off". When the particles are exposed to visible light, the particles redisperse and catalysis can proceed.

Catalytic systems that can be switched "on" and "off" by an external stimulus[1−8] are interesting for controlled drug release/delivery,[1a] as mimicks of regulatory biocatalysts,[2] and in the general context of the development and improvement of synthetic strategies.[3] The use of light as the catalysis-controlling agent is particularly appealing since it can be delivered virtually instantaneously to the whole volume of the sample without any transport (e.g., diffusion) limitations inherent to chemical delivery. Photoswitchable catalysts have been investigated by several groups and have generally been based on molecular switches (e.g., azobenzenes, spiropyrans, dithienylethenes) that control the steric hindrance near the catalytic center and/or its electronic properties. For example, Hecht and co-workers showed that the activity of piperidine catalysts in the Henry reaction can be modulated by covalently attached azobenzenes.[3a,4] Willner's group demonstrated photoswitchable electrocatalysis using photoisomerizable monolayers and Pt nanoparticles.[5] Other notable examples include photomodulated, deoxyribozyme-catalyzed RNA cleavage,[2a] light control of peroxidase activity using quantum dots,[2c] photoswitchable stereoselectivity of a catalytic copper dithienylethene complex,[6] photocatalytic hydrolysis of nitrophenyl acetate by azobenzene-capped cyclodextrins,[7] and conversion of carbon dioxide and propylene oxide into propylene carbonate catalyzed by aluminum porphyrin regulated by the photoisomerization of stilbazole.[8] Notwithstanding the ingenuity of these systems, many of them show modest on-to-off ratios of catalytic activity (2−35.5[1−4,8]), and only in three examples more than one switching event has been demonstrated.[2a,c,5] Here, we consider a conceptually different approach to photoactivated catalysis in which catalytic activity is modulated by approximately 2 orders of magnitude by the dynamic, light-controlled aggregation/dispersion of nanoparticles (NPs).[9] Our model system is based on gold nanoparticles (AuNPs) decorated with a mixture of "background" alkane amines and photoswitchable azobenzene-terminated alkane thiols.[10] In the absence of light, the NPs remain unaggregated, expose a large surface area, and efficiently catalyze a hydrosilylation reaction.[11] Upon irradiation with UV light, however, the NPs aggregate reducing the solvent-exposed surface area and effectively switching the catalysis off. The catalytic activity is regained upon visible irradiation and NP dispersion and can be halted again by UV-induced aggregation.

We used gold nanoparticles (AuNPs; diameter $d_{core} = 5.5 \pm 0.6$ nm, total diameter including the coating organics, $d = \sim 8.0$ nm) synthesized as described before[10b,c] and functionalized with a mixed self-assembled monolayer, mSAM,[10a] of dodecylamine, DDA, and photoswitchable azobenzene-terminated alkane thiols (**AT**: 11-(4-(phenylazo)phenoxy)-1-undecane-thiol), Figure 1A). The surface coverage, χ, of **AT** ligands on the NPs was controlled as described previously[10c,d] and varied from 0.05 to 0.5 (see Supporting Information, SI, Section 1). The NPs were suspended in degassed toluene to which the reagents of the hydrosilylation reaction (4-methoxybenzaldehyde, **1**, and diphenylsilane, **2**) were added under argon. The dispersed AuNPs catalyzed[12] the formation of 4-methoxybenzyloxy-diphenylsilane, **3** (Figure 2A, red curve), with a bimolecular rate constant, $k_{on} \approx 9 \times 10^{-4}$ mM^{-1} min^{-1} estimated from NMR spectra (see SI, Section 4) and using a fitting procedure detailed in ref 13. When, however, the reaction mixture was irradiated with 365 nm UV light (light intensity ≈ 0.05 W/cm^2), the reaction slowed down (typical rate constant, $k_{off} \approx 1 \times 10^{-5}$ mM^{-1} min^{-1}; Figure 2A, blue curve).

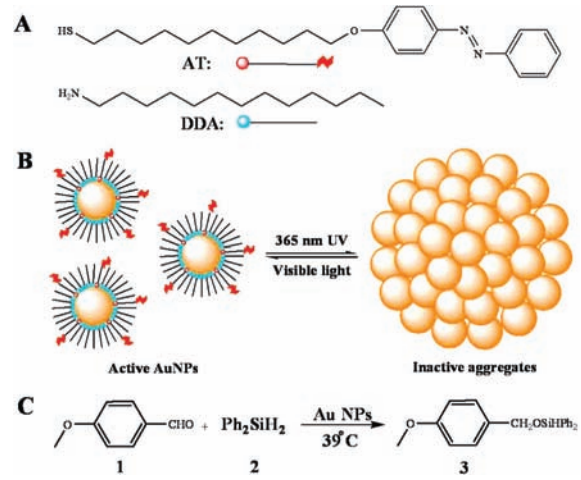

Figure 1. (A) Molecular structures of the "background" DDA surfactant and of the photoresponsive azobenzene-thiol ligand, AT. (B) Schematic representation of a photoswitchable AuNP system. Dispersed NPs are catalytically active; aggregated NPs are catalytically inactive. (C) Hydrosilylation of 4-methoxybenzaldehyde catalyzed by AuNPs in dry toluene at 39 °C and under argon.

Based on these differences, a switchable system was constructed in which the catalysis is switched "on" under irradiation with visible light (white light, light intensity ~0.1 W/cm^2) and is switched "off" when the sample is irradiated with UV. Figure 2B illustrates reaction progress over three "off−on" cycles with the on-to-off ratio of the reaction rate constants in the presence and in the absence of UV irradiation on the order of 90.[14] We note that the curves in Figure 2 do not continue for longer times (i.e., for more than three cycles) to emphasize the fact that UV irradiation becomes gradually less

10.1021/ja104260n

efficient in switching catalysis "off"; the origin of this effect is discussed later in the text.

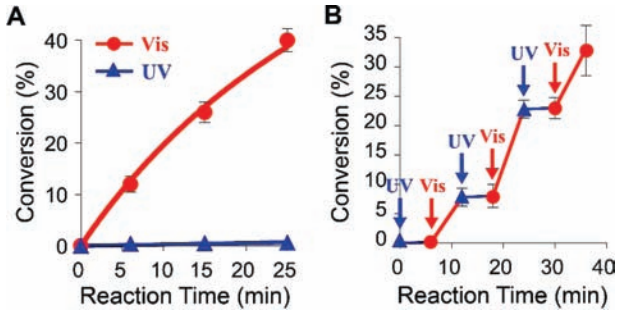

Figure 2. (A) Percent conversion for the AuNP-catalyzed hydrosilylation of 4-methoxybenzaldehyde as a function of time under irradiation with visible light (red markers) and under 365 nm UV irradiation (blue markers). The lines are fits to the kinetic equation derived in ref 13. Surface coverage of azobenze ligands on the AuNPs was $\chi = 0.3$. (B) Hydrosilylation of 4-methoxy-benzaldehyde can be switched "on" by visible light (red portions of the curve) and "off" by UV (blue portions). For the experiments shown, $\chi = 0.31$. Error bars were calculated based on standard deviations from three NP batches, three samples per batch.

The ability to switch catalysis "on" and "off" derives from the reversible aggregation of the functionalized NPs. Specifically, when the NPs are irradiated with UV light, the azobenzene groups of their thiol ligands undergo a *trans*-to-*cis* isomerization and develop ~5 D electric dipoles.[10b,c] In nonpolar solvent, these dipoles translate into attractive forces between the NPs (for typical values of surface coverage, $\chi = 0.3$, ~10 kT per NP pair; see ref 10b) which, in turn, mediate complete aggregation of the particles into larger structures within ~1 min. This process is evidenced by the red shift of the UV−vis spectra of the NP solutions (Figure 3B) as well as by the dynamic light scattering (DLS) measurements (Figure 3C) and TEM imaging (Figure 3A). Based on the DLS and TEM data, the sizes of the aggregates are estimated at $D \approx 900$ nm. The decrease in the rate of catalysis on AuNP surfaces is then due to the decrease of the total solvent-exposed surface area, S, of these particles. Basic geometric arguments[15] indicate that, upon aggregation, the exposed surface area decreases approximately by a factor of $(D/d)\eta$ where η, ~0.64,[16] is the packing fraction of the individual NPs within the aggregate; for the experimental values of NP and aggregate diameters, we have ~74, which is close to the factor by which the reaction rate constants decrease. Such agreement should, indeed, be expected for heterogeneous catalysis,[17] where the reaction rate is known to scale with the number of active/available surface sites per unit mass of the catalyst,[18] ρ. It follows that $k_{on}/k_{off} \approx \rho_{on}/\rho_{off}$. Because the mass of the AuNP catalyst in the unaggregated/"on" and aggregated/"off" states is conserved, the ratio ρ_{on}/ρ_{off} reduces to the ratio of the number of active surface sites $\rho_{on}/\rho_{off} = N_{on}/N_{off}$. Assuming that the distribution of such sites is random with, on average, one site per surface area of A_S, we have $N_{on}/N_{off} = N_{on}A_S/N_{off}A_S = S_{NP}/S_{Agg}$ and, finally, $k_{on}/k_{off} = S_{NP}/S_{Agg}$.[19]

The aggregates forming upon UV irradiation are metastable and disintegrate into individual nanoparticles when the UV irradiation ceases, and the *cis*-azobenzenes reisomerize into the *trans* form having no electrical dipoles mediating interparticle attractions.[20] Reisomerization and aggregate dissolution are markedly accelerated upon irradiation with visible light. UV−vis and DLS measurements illustrated in Figure 3 show that within 1−2 min the aggregates revert to individual NPs; these free NPs are again capable of efficient catalysis.

Several parameters controlling the performance of the system merit further discussion. First, the composition of the mSAM has a pronounced effect on catalysis. If all ligands—both the azobenzene-terminated switches and the alkane-chain "background"—are thiols, no catalysis takes place. This observation is congruent with previous works showing that thiols poison the catalytic gold surface.[21] The amine ligands such as DDA bind to the gold surface more loosely than the corresponding alkane thiols (binding free energies $\Delta G_{DDA} \approx -11.4$ kJ mol^{-1} vs $\Delta G_{thiol} \approx -22.8$ kJ mol^{-1}; see ref 22) and do not hinder catalysis. On the other hand, if all ligands, including the azobenzene switches, are attached to the NPs via weakly binding amines, they are too labile and reversible aggregation−dispersion becomes problematic. We found that the best compromise is to use mixed SAMs incorporating strongly binding thiols serving as switches and weakly binding amines serving as background ligands. For such mixed monolayers, the fraction of azobenzene thiols has to be above ~0.23 to ensure robust light-driven aggregation/dispersion but below 0.33 to not poison the catalyst; in other words, the optimal range for photocatalysis is $0.23 \leq \chi \leq 0.33$.

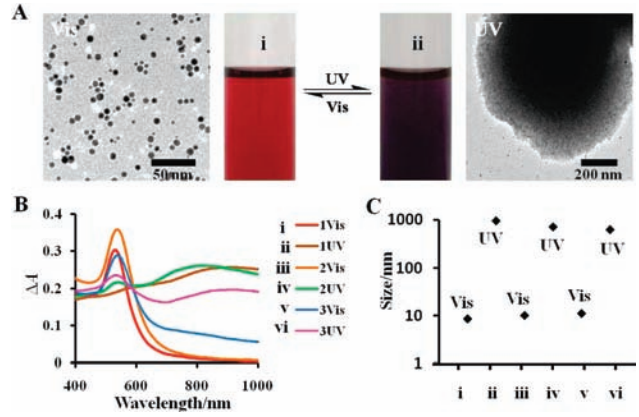

Figure 3. (A) Typical color changes of the reaction mixture irradiated with 365 nm UV (*i* to *ii*) and visible (*ii* to *i*) light. The corresponding TEM images show dispersed and aggregated AuNPs. (B) UV−vis spectra corresponding to the cycles of alternating vis and UV irradiation (from *i* to *vi*, 6 min each). (C) The sizes of free and aggregated AuNPs measured by DLS (note the logarithmic *y*-scale).

The major limitation of photoswitchable catalytic systems reported to date[1−8] is that they can only rarely perform more than one on−off catalytic cycle. In our system, photomodulation of catalytic activity is very efficient over at least three UV−vis cycles (see Figure 2B), but beyond this point not all NPs aggregate upon UV exposure, and the catalysis cannot be completely switched "off" (although the k_{on}/k_{off} ratios remain above ~10 for several more cycles). One possible explanation here could be that the SAMs coating the NPs are being damaged by UV light; however, the light intensities we used, ~0.05 W/cm^2, are similar to those used in other photoswitchable AuNP systems for which many more NP aggregation/dispersion events were achieved (e.g., over ~300 for the nanoparticle based "photopaper"[10c]). Also, the TEM images and the UV−vis spectra of the particles do not change markedly from the first to the second switching cycles ruling out the possibility of particle coalescence.[22] Instead, a reasonable explanation is that both the 4-methoxybenzaldehyde and diphenylsilane substrates of the hydrosilylation reaction have affinity for the gold surface[12b,23] from which they can gradually displace the DDA and, more importantly, the azobenzene thiols. This is all the more likely since these substrates are used in large excess with more than 50 molecules in solution per one ligand (DDA and azobenzene thiols) on the AuNPs.

Lastly, we note that the k_{on}/k_{off} ratios were similar when NPs of other sizes (3 and 10 nm) were used. This observation indicates that nanoparticle curvature has a negligible effect on catalytic activity and the switching mechanism. On the other hand, polar solvents such as MeOH or acetonitrile had a highly detrimental effect on the photoinduced NP aggregation and consequent catalytic behavior, since the dipole−dipole forces in polar solvents are greatly diminished (their strength scales with $1/\varepsilon^2$, where ε is the dielectric constant of the solvent).[24]

In summary, we demonstrated photoswitchable catalysis controlled by reversible aggregation/dispersion of catalytic nanoparticles. While the present system achieves more switching cycles than in most previous works,[1−5] it is clear that for practical applications the number of cycles in which the k_{on}/k_{off} ratio remains high should be increased substantially. This could potentially be achieved by the use of reactions in which reaction substrates/products do not compete with the switchable ligands for the adsorption/catalytic sites on the NPs. In this context, the use of homogeneous catalysts tethered onto the NPs appears most promising and versatile, though it will require avoiding cross-reactivity of these ligands with the functional groups attaching to the nanoparticle surfaces.[25]

Acknowledgment. This work was supported by the Nonequilibrium Energy Research Center (NERC) which is an Energy Frontier Research Center funded by the U.S. Department of Energy, Office of Science, Office of Basic Energy Sciences under Award Number DE-SC0000989.

Supporting Information Available: Experimental details including synthesis of AuNPs, functionalization of AuNPs with mixed DDA/AT SAMs, NMR spectra, and calculation of the percent conversions from NMR spectra. Note: AT ligands were synthesized as described previously.[10c]

This material is available free of charge via the Internet at http://pubs.acs.org.

References

(1) (a) Shrestha, N. K.; Macak, J. M.; Schmidt-Stein, F.; Hahn, R.; Mierke, C. T.; Fabry, B.; Schmuki, P. *Angew. Chem., Int. Ed.* **2009**, *48*, 969–972. (b) Piermattei, A.; Karthikeyan, S.; Sijbesma, R. P. *Nat. Chem.* **2009**, *1*, 133–137. (c) Buyanov, R. A.; Molchanov, V. V.; Boldyrev, V. V. *Catal. Today* **2009**, *144*, 212–218.

(2) (a) Keiper, S.; Vyle, J. S. *Angew. Chem., Int. Ed.* **2006**, *45*, 3306–3309. (b) Wang, G.; Kuroda, K.; Enoki, T.; Grosberg, A.; Masamune, S.; Oya, T.; Takeoka, Y.; Tanaka, T. *Proc. Nat. Acad. Sci. U.S.A.* **2000**, *97*, 9861–9864. (c) Fruk, L.; Rajendran, V.; Spengler, M.; Niemeyer, C. M. *ChemBioChem* **2007**, *8*, 2195–2198.

(3) (a) Peters, M. V.; Stoll, R. S.; Kuhn, A. K.; Hecht, S. *Angew. Chem., Int. Ed.* **2008**, *47*, 5968–5972. (b) Samachetty, H. D.; Lemieux, V.; Branda, N. R. *Tetrahedron* **2008**, *64*, 8292–8300.

(4) (a) Stoll, R. S.; Peters, M. V.; Kuhn, A.; Heiles, S.; Goddard, R.; Buhl, M.; Thiele, C. M.; Hecht, S. *J. Am. Chem. Soc.* **2009**, *131*, 357–367. (b) Stoll, R. S.; Hecht, S. *Org. Lett.* **2009**, *11*, 4790–4793.

(5) Niazov, T.; Shlyahovsky, B.; Willner, I. *J. Am. Chem. Soc.* **2007**, *129*, 6374–6375.

(6) Sud, D.; Norsten, T. B.; Branda, N. R. *Angew. Chem., Int. Ed.* **2005**, *44*, 2019–2021.

(7) (a) Ueno, A.; Takahashi, K.; Osa, T. *J. Chem. Soc., Chem. Commun.* **1980**, 837–838. (b) Ueno, A.; Takahashi, K.; Osa, T. *J. Chem. Soc., Chem. Commun.* **1981**, 94–96.

(8) Sugimoto, H.; Kimura, T.; Inoue, S. *J. Am. Chem. Soc.* **1999**, *121*, 2325–2326.

(9) Fialkowski, M.; Bishop, K. J. M.; Klajn, R.; Smoukov, S. K.; Campbell, C. J.; Grzybowski, B. A. *J. Phys. Chem. B* **2006**, *110*, 2482–2496.

(10) (a) Witt, D.; Klajn, R.; Barski, P.; Grzybowski, B. A. *Curr. Org. Chem.* **2004**, *8*, 1763–1797. (b) Klajn, R.; Bishop, K. J. M.; Grzybowski, B. A. *Proc. Nat. Acad. Sci. U.S.A.* **2007**, *104*, 10305–10309. (c) Klajn, R.; Wesson, P. J.; Bishop, K. J. M.; Grzybowski, B. A. *Angew. Chem., Int. Ed.* **2009**, *48*, 1–6. (d) Because thiols bind onto the gold surface much stronger than DDA (the difference in adsorption equilibrium constant is ca. 2 orders of magnitude; see ref 10c), the surface coverage of azobenzene thiols, ATs, is calculated assuming that these ligands added to the NP solution displace DDA surfactants quantitatively. For example, to obtain fractional surface coverage $\chi = 0.3$, 24.8 μL of 2 mM AT (4.96×10^{-5} mmol) solution is injected into 250 μL of purified, 7.6 mM AuNP solution (corresponding to 1.65×10^{-4} mmol of ligand binding sites on 5.5 nm AuNPs).

(11) Wei, Y.; Soh, S.; Apodaca, M. M.; Kim, J.; Grzybowski, B. A. *Small* **2009**, *6*, 857–863.

(12) (a) Corma, A.; Gonzalez-Arellano, C.; Iglesias, M.; Sanchez, F. *Angew. Chem., Int. Ed.* **2007**, *46*, 7820–7822. (b) Raffa, P.; Evangelisti, C.; Vitulli, G.; Salvadori, P. *Tetrahedron Lett.* **2008**, *49*, 3221–3224.

(13) The reaction catalyzed by the AuNPs can be written as

$$A + B \xrightarrow{k} C$$

where A and B are substrates (4-methoxybenzaldehyde and diphenylsilane, respectively), C is the product (4-methoxybenzyloxy-diphenylsilane), and k is the rate constant of the reaction. Writing the rate equation as $R = dC_C/dt = kC_AC_B$ and denoting the initial concentrations of A and B as $C_{A0} = 20$ mM and $C_{B0} = 25$ mM, we have $R = dC_C/dt = k(C_{A0} - C_C)(C_{B0} - C_C)$. The solution of this first-order differential equation is $C_C = (e^{(C_{A0}-C_{B0})kt} - 1)/(e^{(C_{A0}-C_{B0})kt}/C_{B0} - 1/C_{A0})$. *The value of the rate constant k is then obtained by fitting this kinetic model to the experimental dependence of the concentration of product, C_C, on time (cf. Figure 2,* where percentage conversion is 100 C_C/C_{A0}). This procedure gives the typical rate constant for the "on"/unaggregated state, $k_{on} = 9 \times 10^{-4}$ mM^{-1} min^{-1}, and $k_{off} = 1 \times 10^{-5}$ mM^{-1}min^{-1} for the "off"/aggregated state. Therefore, the on-to-off ratio is $k_{on}/k_{off} \approx 90$.

(14) The same method as that detailed in ref 13 is used in Figure 2B to calculate the reaction rate constants. The first cycle has an average "off" rate constant of 6.7×10^{-6} mM^{-1} min^{-1} and a subsequent average "on" rate constant of 5.5×10^{-4} mM^{-1} min^{-1}. This gives a ratio of $k_{on}/k_{off} \approx 82$. The second cycle has an average "off" rate constant of 1.5×10^{-5} mM^{-1} min^{-1} and an average "on" rate constant of 1.3×10^{-3} mM^{-1} min^{-1}, giving a ratio of $k_{on}/k_{off} = 87$. The third cycle has an average "off" rate constant of 2×10^{-5} mM^{-1} min^{-1} and an average "on" rate constant of 1.2×10^{-3} mM^{-1} min^{-1}, giving a ratio of $k_{on}/k_{off} = 60$.

(15) Consider a spherical aggregate of diameter $D = 2R$ (volume $V = 4\pi R^3/3$) made of randomly-packed (packing fraction $\eta \approx 0.64$, ref 16) spherical NPs, each of diameter $d = 2r$ (volume $v = 4\pi r^3/3$). Because $V\eta \approx n v$, the number of particles in the aggregate is $n \approx (V/v)\eta = (R/r)^3\eta$. The total surface area of the component NPs is then $S_{NP} = n4\pi r^2 = 4(R/r)^3\eta\pi r^2$, compared to the surface area of the aggregate $S_{Agg} = 4\pi R^2$. It follows that the ratio of surface areas is $S_{NP}/S_{Agg} = (R/r)\eta = (D/d)\eta$. Here, $D \approx 920$ and $d \approx 8$ nm, so $S_{NP}/S_{Agg} \approx 73.6$. Note that this is a conservative estimate since it neglects solvent availability of any NPs inside the aggregates; in other words, the real ratio might be slightly lower than 73.6.

(16) Jaeger, H. M.; Nagel, S. R. *Science* **1992**, *255*, 1523–1531.

(17) (a) Bell, A. T. *Science* **2003**, *299*, 1688–1691. (b) Sun, N.; Klabunde, K. J. *J. Am. Chem. Soc.* **1999**, *121*, 5587–5588. (c) Wang, X.; Ning, P.; Liu, H.; Ma, J. *Appl. Catal. B:* **2010**, *94*, 55–63. (d) Haruta, M. *Cat. Today* **1997**, *36*, 153–166.

(18) Fogler, H. S. *Elements of Chemical Reaction Engineering*, 3rd ed.; Prentice Hall: Upper Saddle River, NJ, 1999.

(19) Of course, density of available active sites on the surface of the catalyst, ρ, may vary as a function of time when the reactants adsorb and the products desorb. This variation is expected to follow a typical Langmuir isotherm. However, such an isotherm for adsorption−desorption reaches steady state relatively rapidly and the density of vacant sites can be approximated as constant.

(20) In the absence of electrical dipoles, the thermal noise is sufficient to overcome van der Waals attractions between the NPs and cause dispersion of NP aggregates (for details, see ref 10b).

(21) (a) Nikolaev, S. A.; Zanaveskin, L. N.; Smirnov, V. V.; Averyanoy, V. A.; Zanaveskin, K. L. *Russ. Chem. Rev.* **2009**, *78*, 231–247. (b) Sau, T. K.; Pal, A.; Pal, T. *J. Phys. Chem. B* **2001**, *105*, 9266–9272.

(22) Klajn, R.; Gray, T. P.; Wesson, P. J.; Myers, B. D.; Dravid, V. P.; Smoukov, S. K.; Grzybowski, B. A. *Adv. Funct. Mater.* **2008**, *18*, 1–7.

(23) Corma, A.; Garcia, H. *Chem. Soc. Rev.* **2008**, *37*, 2096–2126.

(24) Bishop, K. J. M.; Wilmer, C. E.; Soh, S.; Grzybowski, B. A. *Small* **2009**, *5*, 1600–1630.

(25) For example, we tried to prepare a system in which Grubbs catalyst would be tethered onto AuNPs. Although numerous synthetic strategies were tested, it proved impossible to attach the catalyst to AuNPs in any appreciable yield and/or with the retention of catalytic activity.

JA104260N